[30]It is assumed τ^{-1} is the same scattering rate as used in the Drude model fit to Al-reflectance data in B. P. Feuerbacher and W. Steinman, Opt. Commun. 1, 81 (1969). (See Table I.)
[31]F. Sauter, Z. Phys. **203,** 488 (1967).
[32]I. Lindau and P. O. Nilsson, Phys. Lett. A **31,** 352 (1970).
[33]M. Anderegg, B. Feuerbacher, and B. Fitton, Phys. Rev. Lett. **27,** 1565 (1971).
[34]R. H. Ritchie and R. E. Wilems, Phys. Rev. **178,** 372 (1969).
[35]Wavefunctions in the region of the image-charge potential were determined from a Runge–Kutta solution of the wave equation.
[36]G. Hass and J. E. Waylonis, J. Opt. Soc. Am. **51,** 719 (1961).
[37]J. G. Endriz and W. E. Spicer, Phys. Rev. B **4,** 4144 (1971).
[38]F. Wooten, T. Huen, and R. N. Stuart, in *Optical Properties and Electronic Structure of Metals and Alloys,* edited by F. Abeles (North-Holland, Amsterdam, 1966), p. 332.
[39]T. F. Gesell and E. T. Arakawa, Phys. Rev. Lett. **26,** 377 (1971).
[40]J. M. Elson and R. H. Ritchie, Phys. Rev. B **4,** 4129 (1971).
[41]This term has been used extensively in the literature, e.g., R. M. Broudy, Phys. Rev. B **3,** 3641 (1971).
[42]C. N. Berglund and W. E. Spicer, Phys. Rev. **136,** A1030 (1964).
[43]This paper concludes that the surface effect is most easily optically detected at energies well below $\hbar\omega_p$ where both s- and p-polarized light are refracted nearly normal to the surface, even for quite high angles of incidence. Light polarization dependence in the photoyield associated with photoexcitation directionality effects (Ref. 19) should thus be strongly subdued at these energies.
[44]A similar method was used to detect surface-plasmon excitation of the surface effect (Refs. 11 and 13). Excitation was reliably calculated in the volume theory and experimental deviations assigned to the surface effect.
[45]This volume effect calculation, $(\mathcal{G}_p/\mathcal{V}_p)Y_{\mathrm{CH:volume}} = \frac{1}{2}\alpha(\phi)l_e(\hbar\omega)y(\hbar\omega)$ corresponds to the lowest-lying volume-effect curve in Fig. 2, Ref. 13. The volume-effect calculations of that reference were based on experimentally observed photoyield, and thus differ from the analytically defined isotropic-excitation model of the present calculation.
[46]Surface-excited electrons emitted into vacuum necessarily escape before they can interact with other electrons. Surface back excited electrons may inelastically scatter back into vacuum, but this process should have a rather low probability.
[47]N. V. Smith and W. E. Spicer, Phys. Rev. **188,** 593 (1969).
[48]Lifetime broadening for Al was calculated from the volume decay theory of Ref. 40 and the optical constants of Table I. The calculated broadening for the reflectance curves of Fig. 13 include effects of coupling to plasmons of different energies as well as lifetime broadening. The photoyield calculation is broadened only by lifetime effects.
[49]A. Bagchi, C. B. Duke, and P. J. Feibelman, Phys. Rev. Lett. **27,** 998 (1971).
[50]R. J. Whitefield and J. J. Brady, Phys. Rev. Lett. **26,** 380 (1971).
[51]J. C. Sutherland, R. N. Hamm, and E. T. Arakawa, J. Opt. Soc. Am. **59,** 1581 (1969); U. S. Whang, E. T. Arakawa, and T. A. Callcott, Phys. Rev. Lett. **25,** 646 (1970).

PHYSICAL REVIEW B VOLUME 7, NUMBER 8 15 APRIL 1973

Resonant Raman Scattering from $Al_xGa_{1-x}As$

Jagdeep Shah, A. E. DiGiovanni, T. C. Damen, and B. I. Miller
Bell Telephone Laboratories, Holmdel, New Jersey 07733
(Received 11 September 1972)

We report the results of a detailed study of resonant Raman scattering from the mixed crystal $Al_xGa_{1-x}As$ at 2 °K using a continuously tunable dye laser. The dye laser enables us to obtain the exact resonance line shape. Comparison of the resonance behavior of the GaAs-like and the AlAs-like LO phonons allows us to determine the energy of the band gap accurately. In addition to the resonance behavior, we have also studied the 1-LO linewidths and line shapes, the behavior of the TO phonon and local modes, and also certain broad luminescence features present in the spectra.

I. INTRODUCTION

Resonant Raman scattering from solids has been investigated rather extensively in the last few years from experimental and theoretical viewpoints.[1] Most of the experimental work until now has been done by using the various discrete lines of different lasers,[1] by varying temperature[2] of the sample, or by applying external perturbations such as magnetic field[3] or stress[4] on the sample. However, the recent advent of pulsed[5] and cw[6] dye lasers provides a very powerful tool for studying the resonance phenomena in Raman scattering from solids. For example, the use of a flashlamp-pumped dye laser enabled us to study in detail the resonant Raman scattering due to bound excitons in CdS.[7] A cw dye laser has been recently used by Cerdeira *et al.*[8] for studying resonance phenomena in germanium.

In this paper we describe our results on resonant Raman scattering from $Al_xGa_{1-x}As$ by using a cw dye laser. We can obtain the exact line shape of resonance by using this technique. Furthermore, this technique enables us to compare the resonance behavior of two different LO phonons (one GaAs-like, another AlAs-like) and provides us with a technique for obtaining the band gap of the material rather accurately. ("GaAs-like" LO phonon is the one whose energy approaches that of the LO phonon in GaAs as x approaches zero.)

It should be mentioned here that GaAs is a direct-gap ($E_g \simeq 1.52$ eV at 2 °K) material, whereas

AlAs is an indirect-gap ($E_g \simeq 2.13$ eV at 2 °K) material. Therefore, increasing the Al content x in $Al_xGa_{1-x}As$ increases the band gap, making the lowest band gap indirect for large x. This direct-indirect transition takes place at x_c, where $x_c \simeq 0.4$.[9] The Γ and the X minima of the conduction band cross each other at x_c. This is expected to lead to some interesting effects in the luminescence spectra and will be discussed at the end of the paper. Finally, it should be mentioned that phonons in $Al_xGa_{1-x}As$ have been studied by infrared absorption[10] and by Raman scattering[11] using the He-Ne and Ar^+ lasers, and that extensive literature exists on the luminescence properties of these alloys.[12] Raman scattering studies of other mixed crystals such as CdS_xSe_{1-x} have also been reported.[13]

II. EXPERIMENTAL TECHNIQUES

The $Al_xGa_{1-x}As$ layers, typically 5–10 μm thick, were grown epitaxially from the liquid phase on the (100) face of Cr-doped n-GaAs. The method used to grow these layers has been described earlier,[14,15] and consists essentially of bringing the seed into contact with a Ga-rich $Al_xGa_{1-x}As$ solution near its liquidus temperature. Although the layers were not intentionally doped, the electron density at room temperature was typically $\sim 5\times10^{16}$ cm^{-3} and the room-temperature mobility was ~ 1500 $cm^2/V\,sec$, as determined by Hall measurements. No p-type layers were studied.

A cw dye laser pumped with an Ar^+ laser was used for the Raman scattering measurements. With Rhodamine 6G dye, the laser could be tuned continuously from ~5700 to 6300 Å. The output power was 10–15 mW and the laser linewidth was ~0.2 Å. A recently proposed output-coupling scheme[16] was used to reduce the fluorescence background of the dye to an acceptable level for Raman scattering studies. The samples were mounted on a copper block immersed in liquid He pumped to 2 °K. All the measurements were made in the backscattering geometry and the scattered signal was dispersed by a double monochromator and detected by a photomultiplier.

III. RESULTS AND DISCUSSION

This section will be divided into four subsections. In Sec. III A we will discuss the resonance-enhancement data, in III B the scattering from local modes and TO phonons, in III C the 1-LO linewidth and line shapes, and in III D certain broad luminescence features associated with the 2-LO scattering.

A. Resonance Enhancement

We will present data for two samples of $Al_xGa_{1-x}As$, with $x=0.43$ and $x=0.48$. The smallest band gaps of both samples are indirect at 2 °K.[12] However, the $x=0.43$ sample is very close to the direct-indirect crossover discussed in the Introduction; i.e., the X minimum of the conduction band is lower than the Γ minimum but the energy difference between the minima $\Delta_{\Gamma X}$ is very small (of the order of or less than the zone-edge phonon energies). For the $x=0.48$ sample, the Γ minimum is higher than the X minimum by several phonon energies.

Figure 1 shows two traces of Raman spectra for $Al_xGa_{1-x}As$ ($x=0.43$) for two different dye-laser wavelengths. LO_1 and LO_2 are the longitudinal-optical phonons which are GaAs-like and AlAs-like, respectively. The incident photon energies in both cases are greater than the band-gap energy, so that TO phonons are not observed.[1] We notice in the figure that the ratio of the intensities of LO_1 and LO_2 shows a dramatic change from ~0.3 to ~2.5 for ~30 Å change in the dye-laser wavelength. This resonance behavior of the scattering intensity is shown as a function of the dye-laser excitation wavelength in Fig. 2 for the LO_1 and LO_2 processes as well as for the 2-LO_1 and LO_1 + LO_2 processes.

Before discussing Fig. 2, it might be appropriate to emphasize a theoretical result. Ganguly and Birman[17] have considered the problem of resonant Raman enhancement in solids with excitons as the intermediate states. They have shown that there are two poles in Raman cross sections. The first ("incident photon resonance") occurs when the *incident* photon energy equals the exciton energy; the second ("scattered photon resonance") occurs when the *scattered* photon energy equals the exciton energy. This is shown very clearly in the calculation for CdS performed by Bendow *et al.*[18]

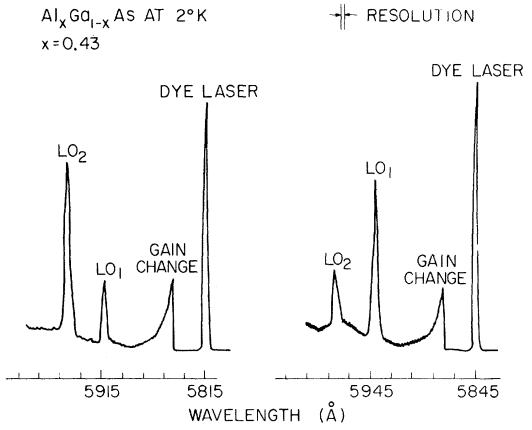

FIG. 1. Unpolarized Raman spectra of $Al_xGa_{1-x}As$ for two different incident photon energies. LO_1 and LO_2 are the GaAs-like and AlAs-like LO phonons, respectively. Notice the change in the ratio of LO_1 to LO_2 intensity.

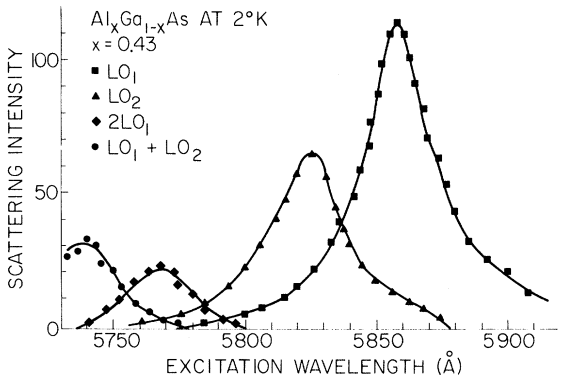

FIG. 2. Normalized scattering intensities of various processes as a function of *incident* photon wavelength. $x = 0.43$.

The existence of the scattered photon pole is also evident in the data of Leite *et al.*[19] We will show below that some of our data can only be explained on the basis of scattered photon resonance. In fact, the use of a material with two LO phonons and a continuously tunable dye laser has enabled us to prove the existence of the scattered photon pole in the clearest manner yet.

There are several features of interest in Fig. 2. First, we note that the curves in Fig. 2 give the exact shape of the resonance enhancement for the various phonon processes. In most of the previous studies on other materials, only a few discrete points were obtained experimentally because lasers used in those studies were not continuously tunable. Second, we note that the resonance enhancement, largest for the GaAs-like phonon, is of the order of 100. The full width (of the resonance) at half-maximum (FWHM) is approximately 30 Å or 10 meV, which is only about a third of the phonon energy. Finally, the processes resonate at different excitation wavelengths. This implies that the resonance is not with the incident photon but with the scattered photon. This last point is made more clearly in Fig. 3, where we have replotted the data of Fig. 2 as a function of the *scattered* photon wavelength. We see that all the maxima in the scattering intensity of various phonon processes occur at the same wavelength of the scattered photon. This confirms that our data show scattered photon resonance and locates the energy of the pole giving rise to the resonance at 5955 Å within ± 5 Å (or less than 2 meV).

One might wonder why we have not observed resonance with the incident photon, which would be expected to occur at dye-laser wavelengths longer than the ones used in Fig. 2. The reason for this is that for such longer excitation wavelengths, the scattered photon falls in the region of strong luminescence and is, therefore, not observable. We will see below that for the $x = 0.48$ sample, for which the direct gap is more than a phonon energy above the indirect gap, we do observe incident photon resonance.

It should now be recalled that no resonance was observed at the indirect gap in GaP.[20] This is physically reasonable for indirect semiconductors in general, at least at low temperatures, since a fifth-order electron-photon interaction is required, in contrast to the usual third-order interaction in direct semiconductors.[21] Thus, although the luminescence studies indicate that this particular sample has an indirect band gap at 2 °K, we attribute the resonance to the *direct* gap or an exciton associated with it. Since the exciton binding energy in this material is expected to be ≈8 meV, the direct band gap is no more than 8 meV above the observed pole energy of 2.082 eV. Thus the direct band gap in this material is determined within an accuracy of ± 6 meV.

Having determined that the observed resonance is due to the scattered photon, we can justify the fact that the absorption corrections were neglected in Figs. 2 and 3. The scattering length is determined by the absorption at the incident photon energy. The variation in the absorption coefficient for incident photon energy greater than the band gap is very slow. Therefore the absorption corrections are negligible over the energy interval of ~10 meV, which is the width of the resonance curve.

Some comments about the resonance line shape might be appropriate here. The resonance line shape is expected to be a Lorentzian when one is so close to one of the intermediate states that contributions to the cross section from all the other

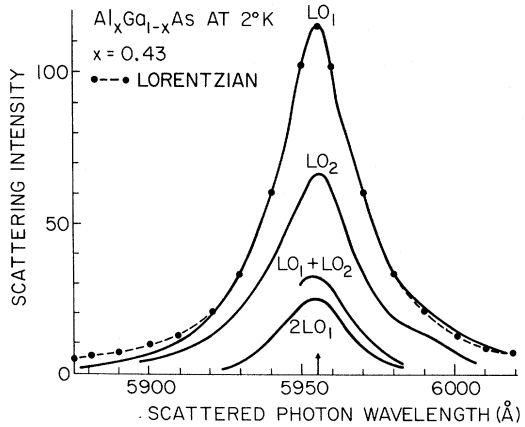

FIG. 3. Normalized scattering intensities of various processes as a function of *scattered* photon wavelength. $x = 0.43$. The solid points are calculated for a Lorentzian centered at 2.082 eV (5955 Å) and having a half-width of 11.2 meV (~32 Å).

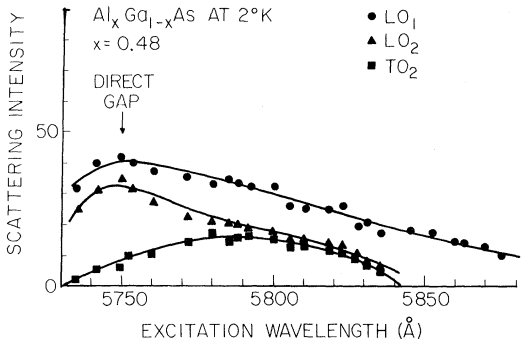

FIG. 4. Normalized scattering intensities vs incident photon wavelength for the $x = 0.48$ sample at 2 °K.

intermediate states may be neglected. In Fig. 3, along with the experimental curves, we have also plotted a Lorentzian whose pole is at 2.082 eV, whose half-width is 11.2 meV, and whose height at peak is taken to be the same as the peak height of the LO_1 process. We can see that the fit between the calculated points and the experimental curve is remarkably good, indicating that a single intermediate state is dominant in our case. The slight asymmetry evident in the data may be dúe to interference between various intermediate states. A detailed investigation of this asymmetry would have been interesting. However, we were unable to carry it out because of strong luminescence bands on one side and the lack of a suitable laser on the other.

We now consider the data for the sample with $x = 0.48$. The direct gap for this sample is considerably higher than that in $x = 0.43$, and the highest photon energy available from our dye laser was just slightly greater than the direct-band-gap energy at 2 °K. Therefore at 2 °K, we could not look for the resonance of the scattered photon. However, the plot of the scattering intensity versus excitation wavelength in Fig. 4 shows the resonance of the incident photon at the direct gap indicated by the arrow. The data in this figure are also uncorrected for absorption. However, unlike earlier figures, absorption corrections are important for this figure, and hence the resonance line shape will be different from the experimental curve in Fig. 4. The reduction in the TO intensity near the band gap is partly an artifact arising from the neglect of absorption and partly a result of the resonance characteristics of the TO phonon in general.[1]

The resonance behavior in the sample with $x = 0.48$ at 165 °K is shown in Fig. 5. Here the peak scattering intensities for the two processes occur at different incident photon energies, as in Fig. 2, indicating that once again we are dealing with scattered photon resonance. From the shift in the pole between 2 and 165 °K, we deduce a band-gap shift of ≈70 meV for the direct gap. This number is entirely reasonable when compared with luminescence measurements.[12] One other point of interest is that the width of the resonance at 165 °K (Fig. 5) is approximately two to three times as large as the width at 2 °K (Fig. 3). Thus, the best measurements of band-gap energies would be obtained at 2 °K, as one would expect.

Finally, we should emphasize here that the sample with $x = 0.48$ has an indirect gap lower than the direct gap with which we observed resonance in Figs. 4 and 5. We have looked for resonance with the indirect band gap but have been unable to find any for either the incident or the scattered photon. These results are consistent with those in GaP,[20] but we must hasten to add that these studies on $Al_xGa_{1-x}As$ were made on thin epitaxial films (~ 5 μm thick). A more careful study on thicker samples, taking into account the absorption corrections accurately, should be performed before ruling out indirect-gap resonances in these materials.

B. Scattering from Local Mode and TO Phonon above Band Gap

In Fig. 6(a) we have plotted the Raman spectra in the vicinity of the 1-LO_1 feature for four different incident wavelengths. These curves are similar to those in Fig. 1, except that these were obtained with higher resolution and show more detail. The trace 1 in Fig. 6(a) shows two weak features. The one close to LO_1 is due to scattering from TO_1 and appears only as a weak shoulder to LO_1. The other broad feature is most likely due to a local mode. The Raman spectra in the vicinity of 1 LO_2 also show a weak feature which is due to TO_2 and a broad feature at lower energies which we

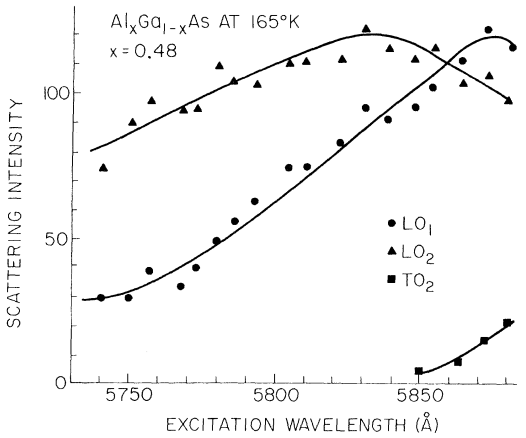

FIG. 5. Normalized scattering intensities vs incident photon wavelength for the $x = 0.48$ sample at 160 °K.

attribute to a local mode. The observation of these local modes is in accord with the observations of Tsu *et al.*[11] However, they observed the local modes only for $x > 0.6$, whereas we observe it for $x = 0.43$ under conditions of resonance.

C. 1-LO Line Shapes

Once again we refer to Fig. 6(a) and note that the 1-LO linewidth (FWHM) is ≈ 0.6 meV (≈ 5 cm^{-1}). This should be compared to ≈ 0.5 cm^{-1} obtained by Chang *et al.*[22] for GaAs at 2 °K. This increased width is not due to inhomogeneity in the value of x.[23] It could, however, be due to decreased lifetime of phonons caused by the increased disorder in the alloy as compared to GaAs.

The second point of interest is the relatively long tail on the low-energy side of the LO_1 Raman lines in the trace 4 of Fig. 6(a). A similar tail is observed for the LO_2 line also. It is well known that the energy of the LO decreases in most materials as the wave vector of the phonon increases, and it appears likely that large-wave-vector LO phonons are responsible for the observed low-energy tail. Large-wave-vector phonons are not observed in Raman scattering from perfect crystals. However, Dean *et al.*[24] have found that disorder in alloys is responsible for the observation of normally forbidden processes (such as no phonon creation of electron-hole pairs or free excitons) in the mixed crystal $GaAs_{1-x}P_x$. This comes about because momentum can be conserved through scattering at impurities. By the same reasoning, Raman scattering by large-wave-vector phonons is possible in a slightly disordered mixed crystal and would account for the observed low-energy tail in our data. We might add here that a similar tail has been observed in thin films of CdS and has been explained on the basis of small crystallites of varying sizes.[25]

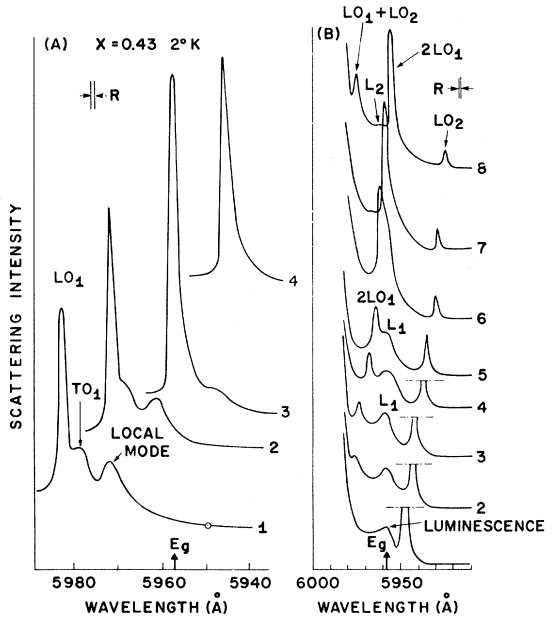

FIG. 6. (a) Spectra in the vicinity of LO_1 for the $x = 0.43$ sample at 2 °K for different incident wavelengths. The TO and the local modes are indicated in the figure. (b) Spectra in the vicinity of 2 LO_1 for the $x = 0.43$ sample at 2 °K for several different incident wavelengths. The luminescence features L_1 and L_2 are indicated. The feature on the extreme right is LO_2 and is not shown fully.

D. Broad Luminescence Features Associated with 2-LO Scattering

In Fig. 6(b) we have plotted several traces of the scattering spectrum near the 2-LO_1 resonance for different values of incident wavelength of the dye laser. The feature at the right is due to LO_2. The 2-LO_1 feature begins to emerge in trace 2 from the strong luminescence tail on the left and passes through resonance in trace 7. The $LO_1 + LO_2$ feature emerges in trace 8 as the incident wavelenth is further decreased.

We would like to focus our attention on the broad features marked L_1 and L_2. These do *not* shift with excitation wavelength, indicating that they are luminescence features. These features occur exactly at the energy of the pole in resonance (see Fig. 2), marked E_g in this figure. The interesting point is that E_g is the energy of the direct band gap or the direct exciton, whereas the lowest band gap of this crystal at 2 °K is indirect, as determined by luminescence studies.[12] The emission from the direct gap when the lowest gap is indirect has been observed at 300 °K in these alloys and can be explained by the long tail in the energy distribution at high temperatures.[12] However, at 2 °K, such an explanation would not be valid. In order to explain this observation, one must assume that some of the electrons somehow get trapped in the higher Γ valley and cannot decay down to the lower X valley of the conduction band. Such a situation would arise if the energy separation $\Delta_{\Gamma X}$ is *smaller* than the energy of the lowest-frequency zone-edge phonon for which intervalley scattering of electrons is allowed. The LA phonon is such a phonon for III-V compounds and its energy in GaAs is 23 meV. From the luminescence measurements and our resonance studies here, we know that $\Delta_{\Gamma X}$ is less than 20 meV. Thus this explanation of the trapping of electrons in the Γ valley is at least plausible in this sample. Further consequences of this interesting situation ($\Delta_{\Gamma X}$ < zone-edge phonon energy) have been discussed by Nguyen and Shah.[26] It should be pointed out here that emission due to resonant impurity states above the direct and indirect band gaps has been previously observed in some other alloys under different conditions.[27]

We conclude this section by noting that this emission L_1 (and L_2) is rather weak and is observable only when the scattered 2-LO processes (either 2 LO, or $LO_1 + LO_2$, or 2 LO_2) occur at energies slightly below E_g. No such emission is seen, for example, in trace 1 or 4 of Fig. 6(b). The reason for this may be that when a photoexcited electron is created slightly less than 1-LO energy above the Γ minimum, one cannot distinguish between luminescence and Raman scattering. However, when an electron is created slightly less than 2-LO energy above the Γ minimum, it can decay to the minimum by simultaneous emission of two large-wave-vector phonons which have lower energy. This process is expected to be very weak. Moreover, it has to compete with rather strong one-phonon intervalley scattering. It is therefore not surprising that the luminescence process L_1 and L_2 are weak.

IV. SUMMARY AND CONCLUSIONS

We have presented resonant Raman scattering data for two different compositions of $Al_xGa_{1-x}As$, obtained by using a continuously tunable cw dye laser. This enabled us to obtain the exact resonance line shapes and compare the behavior of GaAs-like and AlAs-like LO phonons. We have demonstrated how the technique of resonant Raman scattering can be used to determine the band gaps rather accurately, and also the usefulness of the cw dye laser as a tool in spectroscopy.

We have also discussed the behavior of TO phonons, the local-mode phonons, and certain broad luminescence features. We have also observed that the width of the LO phonons in alloys differ from those in pure crystals like GaAs and that a tail is present on the low-energy side of the phonon spectrum. We have suggested that disorder in the alloys may be responsible for both these phenomena. We have also discussed the possibility that a very small energy difference between the Γ and the X valleys might lead to some interesting effects, including the observation of the broad luminescence features in the spectrum.

One unresolved problem is whether or not there is a resonance with the indirect gap. Our data are not definitive on this point because of thin epitaxial layers used in this work. It would be useful to repeat these measurements on bulk-grown materials so that accurate absorption correction may be made.

ACKNOWLEDGMENTS

We would like to thank P. K. Tien and R. J. Martin for the loan of their argon laser, R. M. Martin for a useful discussion, and W. F. Brinkman and J. F. Scott for valuable comments on the manuscript.

---

[1]A survey of the early work on resonant Raman scattering is given by J. F. Scott, R. C. C. Leite, and T. C. Damen, Phys. Rev. 188, 1285 (1969).

[2]J. F. Scott, T. C. Damen, W. T. Silfvast, R. C. C. Leite, and L. E. Cheesman, Opt. Commun. 1, 397 (1970).

[3]T. C. Damen and Jagdeep Shah, Phys. Rev. Letters 26, 249 (1971).

[4]E. Anastassakis and F. H. Pollak, Bull. Am. Phys. Soc. 17, 327 (1972).

[5]P. P. Sorokin and J. R. Lankard, IBM J. Res. Develop. 11, 148 (1967).

[6]O. G. Peterson, S. A. Tucio, and B. B. Snavely, Appl. Phys. Letters 17, 245 (1970).

[7]T. C. Damen and Jagdeep Shah, Phys. Rev. Letters 27, 1506 (1971).

[8]F. Cerdeira, W. Dreybrodt, and Manuel Cardona, Solid State Commun. 10, 591 (1972).

[9]H. C. Casey and M. B. Panish, J. Appl. Phys. 40, 4910 (1969).

[10]M. Ilegems and G. L. Peterson, Phys. Rev. B 1, 1576 (1970).

[11]R. Tsu, H. Kawamma, and L. Esaki, Bull. Am. Phys. Soc. 17, 326 (1972).

[12]See, for example, Jagdeep Shah, B. I. Miller, and A. E. DiGiovanni, J. Appl. Phys. 43, 3436 (1972).

[13]See, for example, session F, in *Proceedings of the International Conference on Light Scattering Spectra of Solids*, edited by G. B. Wright (Springer-Verlag, New York, 1969), pp. 439–476.

[14]M. B. Panish, S. Sumski, and I. Hayashi, Met. Trans. 2, 795 (1971).

[15]B. I. Miller, E. Pinkas, I. Hayashi, and R. Capik, J. Appl. Phys. 43, 2817 (1972).

[16]Jagdeep Shah, Appl. Phys. Letters 20, 479 (1972).

[17]A. K. Ganguly and J. L. Birman, Phys. Rev. 162, 808 (1967).

[18]B. Bendow, J. L. Birman, A. K. Ganguly, T. C. Damen, R. C. C. Leite, and J. F. Scott, Opt. Commun. 1, 267 (1970).

[19]R. C. C. Leite, J. F. Scott, and T. C. Damen, Phys. Rev. Letters 22, 780 (1969).

[20]J. F. Scott, T. C. Damen, R. C. C. Leite, and W. T. Silfvast, Solid State Commun. 7, 953 (1969).

[21]See, for example, J. M. Ralston, R. L. Wadsack, and R. K. Chang, Phys. Rev. Letters 25, 814 (1970).

[22]R. K. Chang, J. M. Ralston, and D. E. Keating, in Ref. 13, p. 369.

[23]From the known variation of the phonon energies with x, we estimate that it would require an inhomogeneity of $\Delta x \approx 0.1$ to account for the observed linewidth. The epitaxially grown layers used in these experiments do not have inhomogeneity of this magnitude, as can be seen from the luminescence data of Ref. 12.

[24]P. J. Dean, G. Kaminsky, and R. B. Zetterstrom, Phys. Rev. 181, 1149 (1969).

[25]T. C. Damen and J. F. Scott, Opt. Commun. (to be published).

[26]Patent application filed by Van-Tran Nguyen and Jagdeep Shah.
[27]D. R. Scifres, N. Holonyak, Jr., C. B. Duke, G. G. Kleinman, A. B. Kunz, M. G. Craford, W. O. Groves, and A. H. Herzog, Phys. Rev. Letters 27, 191 (1971).

PHYSICAL REVIEW B VOLUME 7, NUMBER 8 15 APRIL 1973

Hydrodynamic Theory of Surface-Plasmon Dispersion

J. Heinrichs*
Institut für Festkörperforschung der Kernforschungsanlage, Jülich, 517, *Jülich, West Germany*
(Received 18 September 1972)

The dispersion of surface-plasma oscillations is calculated analytically, using the Bloch hydrodynamic model for an electron gas and solving Maxwell's equations in the absence of retardation effects. This study is based on an approximation for a constitutive relation which provides a useful alternative to previous model descriptions of the surface. It is found that at long wavelengths the surface-plasmon dispersion relation includes a term which is linear in the momentum parallel to the surface and which is half as large as in the case of a study for specular reflection. In contrast to hydrodynamic treatments for specular reflection, the present one leads to an appreciable Landau damping of the surface-plasma oscillations. The magnitude of this Landau damping is roughly consistent with the results of a recent numerical study of plasmons for a more realistic model of the surface. Also discussed in some detail are the charge-density fluctuations associated with the surface plasmon, and a useful relation is established between the amplitudes of bulk- and surface-charge oscillations. In an appendix it is shown that when the imaginary part of the hydrodynamic dielectric function is neglected, one is led to surface modes which are quite different from the usual surface plasmon. Finally the results for surface plasmons are compared with those which are obtained for surface phonons in a metal film and the relationship between two different recent analyses of the surface-phonon problem is discussed in some detail.

I. INTRODUCTION

The dependence of the surface-plasmon frequency on the momentum parallel to the surface of a semi-infinite electron gas is potentially interesting, because of its sensitivity to the details of the electronic properties of the surface. Although experimental data on the dispersion of surface plasmons are scarce, many theoretical studies of this effect have appeared in recent years.[1–12]

The models which have been used in detailed analyses do not differ significantly as far as the description of the surface is concerned. Both in classical or semiclassical and in fully quantum-mechanical treatments, the surface is usually idealized as a perfectly reflecting well-defined boundary, from which the electrons are scattered specularly. In the classical and quasiclassical theories, the unperturbed electron density is assumed to be constant in the occupied space right up to the surface, at which it falls off abruptly to zero. The additional assumption—namely, that in the presence of an induced density fluctuation, all the particles which strike the surface are reflected specularly—then enters as a boundary condition for the perturbed electron distribution function. In first-principle quantum-mechanical treatments, the condition of specular reflection is automatically incorporated by describing the surface by means of an infinite potential step which terminates the unperturbed potential of the bulk. In this model the equilibrium electron density may vary because of quantum-mechanical interference between incoming and reflected particle waves. Both the quasiclassical and quantum-mechanical treatments may be referred to as "sharp-surface models" in the sense that, in both cases, the perturbed electron density is forced to vanish outside a suitably placed effective surface.

Recently, however, Bennett[13] and Beck and Celli[14] have presented two different numerical calculations of the surface-plasmon dispersion relation which go beyond the simple sharp-surface model. Bennett[13] treats a surface where the electron density falls off to zero from its bulk value over a finite width in the surface region, using the hydrodynamic model for the electron gas. The quantum-mechanical calculation of Beck and Celli[14] starts out from an appropriate finite-step surface potential, to which the electrons are allowed to adjust self-consistently in an approximate way. The results of these recent studies differ strongly from those of the earlier calculations[2–4,9–11] and are in much closer agreement with the available data, as